Reverse Bias Behavior of Surface Mount Solid Tantalum Capacitors

Alexander Teverovsky, Ph.D.
QSS Group, Inc./NASA

1. Introduction

1.1. Background.

Solid tantalum capacitors are polarized devices designed to operate only under forward voltage bias conditions. Application of reverse voltage may produce high leakage currents with potentially destructive results. Such misapplications of these devices sometimes occur during bench testing, troubleshooting of engineering modules and/or during some malfunctions in operating systems. However, more serious consequences of reverse bias application are caused by incorrect installation of the capacitor on the board.

In practice, the situation sometimes arises where assembled hardware is suspected of having one or more solid tantalum capacitors installed backwards. Verification of this problem is often complicated by the expense of disassembling hardware for close inspection. In these situations, program managers would benefit from a risk assessment that predicts possible consequences of reverse installation in the intended application and the probability of failures in the system within the mission operation time. Unfortunately, there is only limited published research regarding the ability of solid tantalum capacitors to survive such conditions. The manufacturers of solid tantalum capacitors provide very conservative guidelines regarding momentary reversals of polarity with no guarantee of performance under prolonged exposures to reverse voltages.

In this work, we explore the behavior of three lots (20 V, 35 V and 50 V rated) of solid tantalum chip capacitors from one manufacturer under various reverse bias conditions.

Content of the paper:

1.2. Summary of Published Guidelines and Research

Existing military specifications for surface mount solid tantalum capacitors (MIL-PRF-55365) do not address the issue of survivability of tantalum capacitors in reverse bias conditions. Users are left to consult guidelines offered by major manufacturers of tantalum capacitors. Generally speaking, these guidelines tend to be highly conservative so as not to imply any guarantee of performance when the user misapplies the device. Common guidelines offered

indicate that these capacitors can withstand reverse voltages equal to 10% to 15% of the forward DC voltage rating at room temperature. When ambient temperature increases, this voltage is reduced typically to 3%-5% at 85°C and to 1% at 125°C. One manufacturer seems to be especially concerned about the reverse bias conditions limiting the peak reverse voltage to 10% of V_R or to 1V max at 25 °C, 3% of V_R or 0.5V max at 85°C and 1% of V_R or 0.1V max at 125°C. The manufacturers emphasize that these ratings cover only exceptional conditions of small level excursions into incorrect polarity and are not intended to cover continuous reverse voltage operation.

The probability of failures of incorrectly installed solid tantalum capacitors has long been an issue in the aerospace community. G. J. Ewell from The Aerospace Corporation addressed this issue in 1984 by analyzing behavior of hermetically sealed metal case solid tantalum capacitors under reverse bias conditions [1]. He found that a long-term reverse bias exposure considerably increases the device leakage current measured under forward bias condition, but does not significantly affect the capacitance and dissipation factor. Some lots of 35 V and 50 V rated capacitors survived 200 and even 8900 hours of reverse bias testing (RBT) at voltages up to 40% of rated voltage (V_R). However, the survival rate was not 100% and the behavior was judged to be lot related.

The conclusion made by G. J. Ewell that the existing manufacturer guidelines are extremely conservative concurs with the results of the testing performed at Hughes in 1988 [2]. In that work it was shown that some capacitors could withstand reverse voltage up to 25% of V_R with very little degradation occurring below 15% of V_R. In all cases healing began to occur after 5 minutes of the application polarity being corrected. These experiments suggested that while solid tantalum capacitors can survive substantial reverse bias without failure, this behavior significantly varies from manufacturer to manufacturer.

Solid tantalum capacitors have been widely used in electronics, including military and aerospace applications, for more than 20 years. However, the processes of the reverse voltage bias degradation are still not yet completely understood. The physical origin of reverse voltage currents and mechanisms of failures under reverse bias conditions in solid tantalum capacitors have been analyzed by several groups of researchers.

I. Bishop and J. Gill from AVX Corp. [3] believe that the reverse-bias failures are due to high density currents flowing through very small areas of microcracks or other defects in the dielectric layer. This results in creation of hot spots in the amorphous tantalum pentoxide and causes its conversion into the more conductive crystalline form. The crystallization can eventually cause a short circuit failure of the capacitor. According to this model one might expect a correlation between the forward and reverse currents, which most likely are flowing through the same defects. However, no such correlation was observed and failures under reverse bias conditions could not be predicted based on any forward or reverse bias measurements. It was found that the reverse voltage behavior of tantalum capacitors is similar for different manufacturers, but varies significantly from lot to lot.

A model explaining rectifying properties of Ta capacitors was suggested by Sikula, et al. at the 2001 Capacitor and Resistor Technology Symposium (CARTS) [4]. The model considered a tantalum capacitor as a metal-insulator-semiconductor (MIS) structure with the tantalum being the metal, tantalum pentoxide being the insulator and manganese oxide being the semiconductor. The rectifying is due to formation of depletion or inversion layers in the semiconductor at the MnO_2 / Ta_2O_5 interface. The forward bias leakage current in the capacitor is due to electrons flowing through traps in the Ta_2O_5 layer and is limited by a barrier at the $MnO_2 - Ta_2O_5$ interface. This forward leakage current has an activation energy of 0.3 eV to 0.6 eV. Under reverse bias conditions and voltages above 1.5V, the barrier virtually disappears thus significantly increasing the reverse current, which in this case has an activation energy between 0.7 eV to 1.1 eV. However, the time evolution of the currents in this model was not considered.

Y. Pozdeev-Freeman explained rectifying in solid tantalum capacitors by structural differences at the Ta / Ta_2O_5 and Ta_2O_5 / MnO_2 interfaces [5, 6]. According to this model, conductive TaO particles that form at the Ta-Ta_2O_5 interface act as spikes concentrating electrical field in the dielectric thus significantly increasing injection of electrons from the tantalum cathode.

There is no current consensus even on the nature of conduction in the tantalum pentoxide layers. Some authors assume that the conduction is due to ionic currents [7, 8] while others suggest that it is due to electron transport either by a Pool-Frenkel mechanism [9] or by a trap hopping mechanism [10].

The purpose of this work was to gain more insight into the nature and physical origin of electrical conduction in tantalum capacitors and to analyze degradation processes in the surface mount parts under reverse bias conditions.

2. Experimental

Three groups of surface mount CWR09 type tantalum capacitors manufactured by one supplier and described in the following table were chosen for the experiments.

Capacitor	VR	Lot DC
22 uF	20 V	9804
6.8 uF	35 V	9821
4.7 uF	50 V	9822

All capacitors were screened to the military specifications thus providing high confidence in the quality of the parts used in our experiments.

A number of experiments were carried out at different voltages and temperatures to characterize short-term and long-term evolution of the leakage currents under reverse bias conditions.

Polarization and depolarization currents (currents in a biased and in a short circuited capacitor) measured at different voltages and temperatures as well as frequency dependencies of C and ESR were used to investigate degradation mechanism during reverse bias stresses. Figure 1a shows schematics of a circuit used for measurements of the polarization and depolarization currents in capacitors. Typically a limiting resistor of R = 10 Ohm was used to restrict inrush currents in the capacitors. At this value of R, the discharge currents in capacitors became negligible and charge currents stabilized after a few milliseconds. This means that the polarization and depolarization currents observed at times of more than 10 to 100 milliseconds are due to the processes of charge redistribution within the tantalum pentoxide layer of the capacitors.

To analyze degradation in solid tantalum capacitors the parts were subjected to multiple reverse bias cycling (RBC) with each cycle including reverse bias stress (RBS) followed by forward bias measurements (FBM). Leakage currents were monitored on capacitors during both RBS and FBM periods.
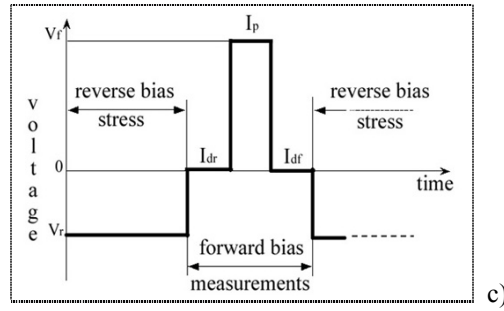

a)

b)

 c)
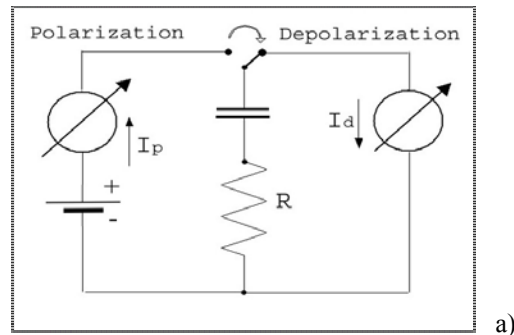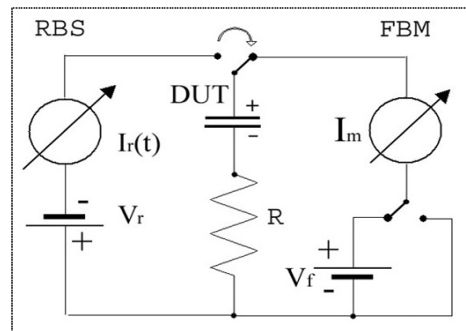
Figure 1. Schematics for (a) measurements of polarization and depolarization currents and (b) for reverse bias cycling (RBC) test. Figure 1c illustrates the voltage diagram during the RBC test, which consists of reverse bias stress followed by forward bias measurements.

The FBM included measurements of currents during depolarization, I_{dr}, forward bias polarization, I_p, and repeat depolarization, I_{df}. Figures 1b and 1c illustrate a test circuit and a time diagram for this technique. The duration of the first RBS period was typically 1000 seconds and these periods were increased with logarithmical increments in the following cycles. Typically from 11 to 20 cycles were performed during each test which resulted in the total reverse-bias times from 20 to more then 250 hours. The duration of each depolarization and polarization period during FBM was 330 seconds.

3. Results

### 3.1. Forward Bias Leakage Current Characterization

The forward bias characterization was performed in an attempt to understand conduction mechanisms in tantalum capacitors.

A characteristic feature of the forward bias leakage currents in tantalum capacitors is their decay with time after applying voltage. Typical I-t curves of forward bias leakage currents at various voltage levels are shown in Figure 2 for the three groups of capacitors. At relatively low voltages, below 10V to 20V, forward leakage currents follow the power law, $I_F \sim t^{-n}$ with the exponent n varying from 0.75 to 0.9 for polarization times up to 30 minutes. At higher voltages there is a tendency for current saturation with time. This behavior suggests that the forward currents are a sum of the absorption current, which varies with time according to the power law, and the conductivity current, which does not depend on time. Similar behavior of forward bias leakage currents is well known for solid tantalum capacitors [11].

In our experiments the absorption currents did not vary significantly from sample to sample. However, the conductivity currents in different capacitors varied more than an order of magnitude.

Depolarization currents at low voltage levels also tend to decrease with time roughly according to the power law. Notably, the absolute magnitude of the polarization and depolarization currents are nearly the same when measured at relatively low voltage levels.

Figure 3 shows polarization and depolarization characteristics measured at relatively low voltages for 35V and 50V rated capacitors, and at rated voltage for a 20 V capacitor in the temperature range from 20 °C to 150 °C. At low voltages and/or temperatures, when the conduction currents are negligible, the polarization and depolarization currents are closely related. An increase in temperature from 20 °C to 100 °C caused an increase in absorption currents of approximately one order of magnitude and virtually did not change the rate of decay (the n value). At temperatures above 100 °C the depolarization currents tended to saturate.
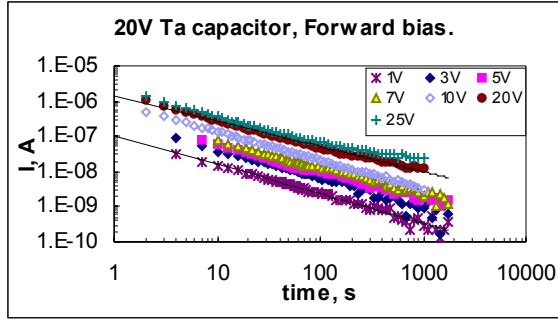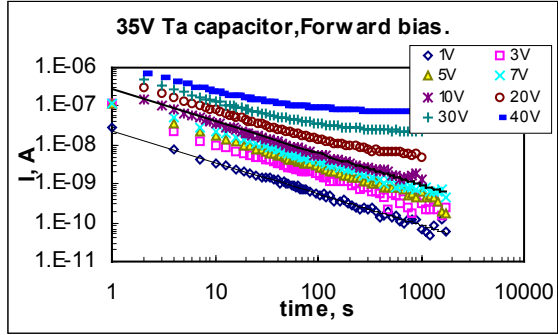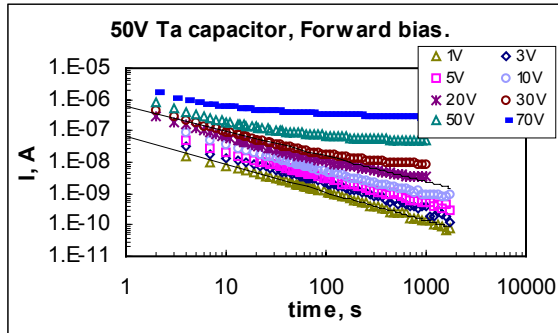
Figure 2. Typical room temperature current decay at different forward voltages for 20V (a), 35V (b) and 50V(c) capacitors. The lines show approximation of the current relaxation according to the power law with the power n = 0.73-0.83 in (a), n = 0.81 in (b) and n = 0.81 – 0.89 in (c).

The observed data suggest that absorption currents are due to the hopping transport mechanism [10]. A simplified model for electron hopping transport predicts that for a trap distribution that is uniform in energy, the current should decay reciprocally with time [12]. Retrapping of electrons and widening of the trap energy distribution would cause deviation from the simple t^{-1} model. This is the most likely reason why we found the exponent to be less than 1 in our experiments.
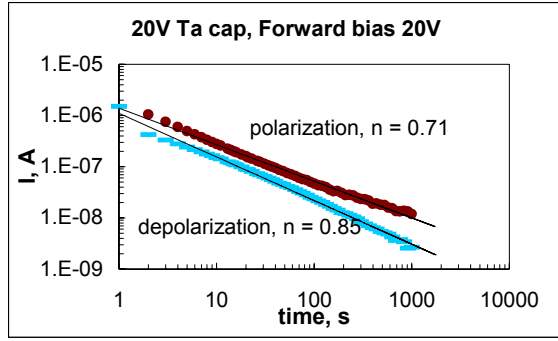
a)
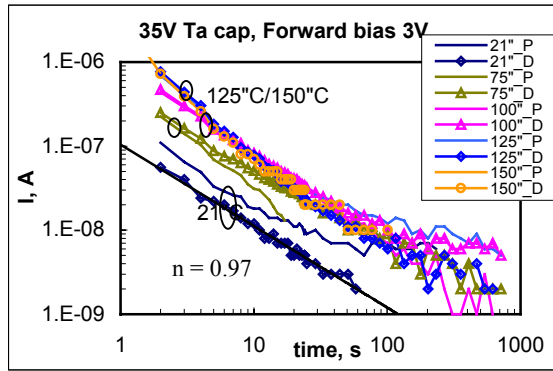
b)
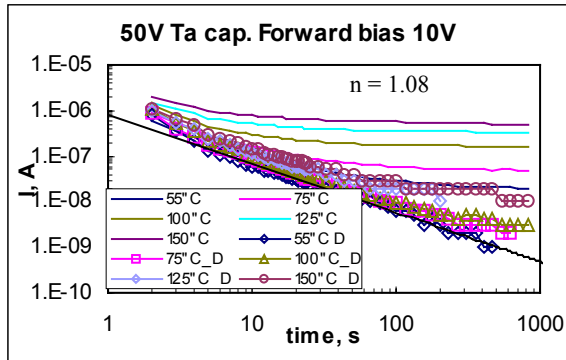
c)

Figure 3. Comparison between polarization and depolarization currents for 20V (a), 35V (b) and 50V (c) capacitors. In figures b) and c) marks indicate depolarization currents and lines indicate polarization currents.

The density of the traps, N_t, can be estimated by the value of the absorbed charge in the capacitor, Q_a as follows:

$$N_t = \frac{Q_a}{qA} = \frac{\int I_d(t)dt}{qA} \quad,$$

where q is the charge of an electron;
A is the volume of the oxide layer;
$I_d(t)$ is the depolarization current.

The volume of the tantalum pentoxide A can be estimated considering that during formation the oxide growth rate, β, is approximately 1.7 to 2.2 nm per volt and that the formation voltage is approximately 3 to 4 times larger than the rated voltage, V_R. With these assumptions, the thickness and the effective surface area of the oxide film in a capacitor can be calculated as:

$$d = \beta \times m \times V_R$$, where m is the formation voltage constant, m =3 – 4.

$$S = \frac{d \times C}{\varepsilon \times \varepsilon_0}$$, where ε is the dielectric constant of tantalum pentoxide (ε = 27) and ε_0 = 8.85 10^{-12} F/m is the

permittivity of free space.

We observed that exposing solid tantalum capacitors to elevated ambient temperature and forward voltages resulted in saturation of depolarization currents at T > 100 °C and applied voltages close to V_R. By these reasons depolarization currents at 150°C after forward bias polarization at rated voltages were used to estimate the N_t values. Results of these calculations, which are displayed in Table 1, suggest that the trap density $N_t \approx 10^{18}$ cm^{-3} and does not depend significantly on the type of capacitor. This value is in agreement with the estimations of trap density in tantalum pentoxide films made by S. Khanin [13].

Table 1. Estimated characteristics of tantalum pentoxide films.

C, µF	V_R, V	d, nm	S, cm^2	V, cm^3	N_t, cm^{-3}
22	20	140	129	1.80E-03	8.6E+17
6.8	35	245	70	1.71E-03	6.3E+17
4.7	50	350	69	2.41E-03	1.2E+18

Leakage currents in the 20V capacitors were mostly due to charge absorption caused by electron hopping through the oxide traps. This mechanism was dominant even at high temperatures (150 °C) and applied voltages (20V), suggesting that the conductivity currents were less than a few nanoamperes. However, for the 35V and 50V capacitors a substantial portion of the leakage current, especially at high temperatures and voltages, was due to the conductivity of the oxide layer. This allowed for analysis of the I-V characteristics of the conduction currents. Figure 4 shows typical current - electric field characteristics for the 50V tantalum capacitors measured at high temperatures. The characteristics indicate a Pool-Frenkel conduction which can be described as follows:

$$I = BE \exp\left(-\frac{U}{kT}\right)\exp(\alpha E) \quad ,$$

$$\alpha = \frac{q^{3/2}}{kT(\pi\varepsilon\varepsilon_0)^{1/2}}$$

where B is a trap-density related constant;
    E is the electric field;
    U is the activation energy;
    k is the Bolzman constant;
    T is the absolute temperature;
    α is a constant equal to the slope of the line in the Pool-Frenkel coordinates.

Estimations of the slope α in Figure 4 gave values from 0.0017 (V/cm)$^{-0.5}$ at 75 °C to 0.0033 (V/cm)$^{-0.5}$ at 175 °C. Calculations per the above equation yields α = 0.0048 (V/cm)$^{-0.5}$ and 0.0037 (V/cm)$^{-0.5}$ respectively at 75 °C and 175 °C. Considering rough estimations used for calculations of the electrical field and possible effect of polarization currents, the agreement between experimental and theoretical data seems reasonable.
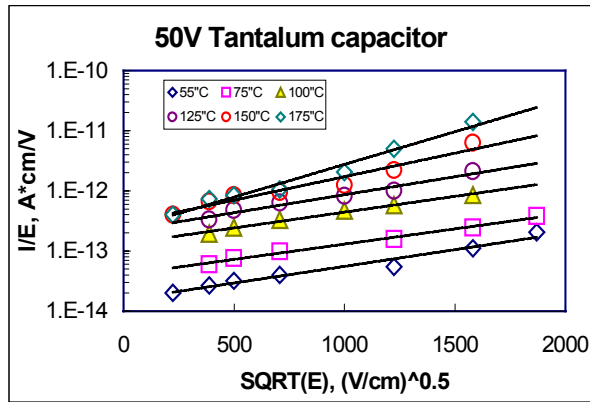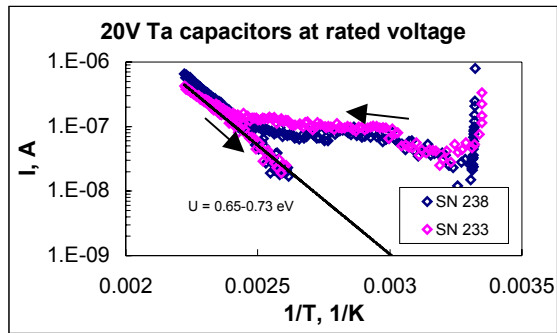
50V Tantalum capacitor

Figure 4. Pool-Frenkel plot of the current - electrical field, E, data calculated at different temperatures for a 50V capacitor.

Typical temperature dependencies of forward leakage currents plotted with Arrhenius coordinates are shown in Figure 5.

a)
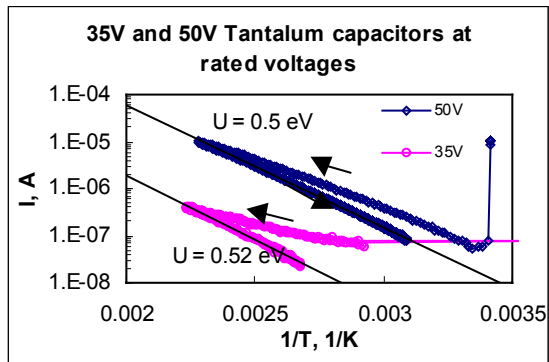
b)

Figure 5. Temperature dependencies of forward currents for 20V (a) and 35V/50V (b) capacitors at rated voltages in the range from 20 °C to 175 °C. The observed hysteresis is due to current relaxation.

These measurements were performed during heating up to 175 °C and then cooling at a rate of 4 °C/min. An initial sharp drop in the current was due to the current decay after applying 50V at room temperature. With decreasing temperature the currents decreased exponentially allowing for estimation of activation energy. Measurements on 50V and 35V tantalum capacitors gave close activation energies of U = 0.5 eV to 0.52 eV. The 20V capacitors had higher activation energies of 0.65 eV to 0.73 eV. Extrapolation of the curves shown in Figure 5a to room temperature gave leakage currents for the 20V capacitors below 0.1 nA. This result confirms that for the 20V capacitors the currents observed at room temperature were mostly due to charge absorption at traps in the tantalum pentoxide film.

Note that the currents measured at increasing temperatures could also be straightened in the Arrhenius plot resulting in lower activation energies of 0.25 eV to 0.4 eV. This is due to a component of the leakage current caused by the charge absorption (polarization) which has relatively weak temperature dependence. This might partially explain the wide variation of the activation energies reported in literature.

3.2. Reverse Bias Currents at low voltages

Reverse bias currents were measured on groups of 3 to 5 capacitors from each of the three lots at test voltages in the range of 1 V to 5 V. The reverse current characteristics (I vs. t) were similar for different samples from the same group. Figure 6a shows an example of reproducibility of these characteristics for 50 V capacitors. At room temperature and reverse voltages below 2V, similar to the forward bias conditions, the reverse leakage currents in all groups of capacitors decreased with time according to the power law with the exponent, n, varying from 0.8 to 1.1. At higher reverse voltages the leakage current increases with time following a relatively short period of current decrease.

Figure 6b shows forward and reverse I-V characteristics of the capacitors with leakage currents measured after 100 seconds of polarization. The I-V characteristics for the three groups of capacitors were similar with somewhat higher currents for the 20V capacitors. This suggests that the absorption currents, which dominate for short polarization times, were similar for different types of capacitors.

The effect of temperature on reverse bias polarization and depolarization currents measured at 2V is shown for a 35V capacitor in Figure 7. Similar to forward bias conditions, at low temperatures, below 75 °C, polarization and depolarization currents were closely related and followed the power law indicating that the same electron hopping mechanism of conductivity is also dominant under low voltage, low temperature reverse bias conditions. At temperatures above 75 °C, polarization currents became much larger than depolarization currents and manifested an increasing-with-time trend. Additional measurements showed that at high temperatures this upward I(t) trend was observed even at reverse bias voltages as low as 1V.

a)
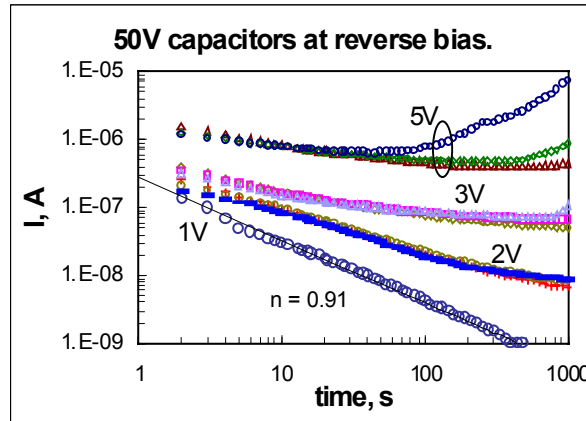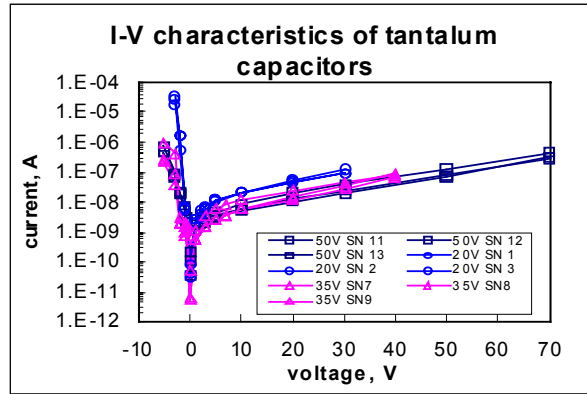
Figure 6. Reverse currents in 50V capacitors (a) and 100-second I-V characteristics of different groups of capacitors (b).
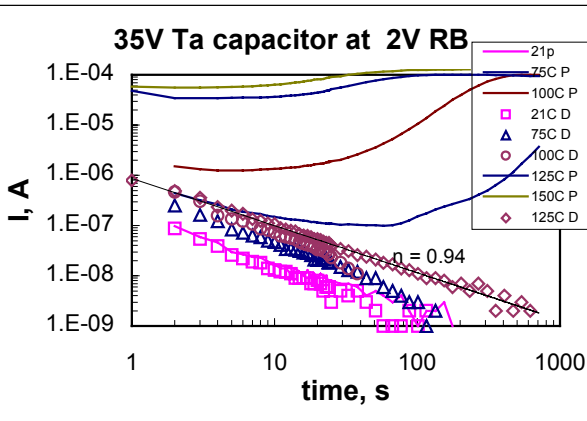

Figure 7. Polarization (lines) and depolarization (marks) currents in a 35V capacitor at 2V of reverse bias and temperatures from 20 °C to 150 °C.

To check the reproducibility of reverse-bias currents, reverse- and forward-bias measurements were repeated after depolarization for 1000 seconds. Figure 8 shows typical results of the repeat measurements obtained for the 50V capacitors polarized at 5V of reverse bias. Repeatable forward and reverse characteristics were observed in all three capacitor ratings after a relatively low-voltage (below 5V) and short (less then a few hours) reverse bias polarization.

Figure 8. Typical curves showing reproducibility of reverse bias I-t characteristics of tantalum capacitors.

Temperature variations of reverse currents were measured during heating up from room temperature to 175 °C and then cooling to approximately 75 °C in one 35V and one 50V capacitor at 2V. Results of these measurements are shown in Figure 9. The observed hysteresis was approximately 3 to 4 orders of magnitude and was due to the reverse currents increasing with time. Similar to the forward bias conditions, at high temperatures variations of reverse currents followed the Arrhenius law with activation energy of 0.4 eV– 0.42 eV.

Figure (50V Tantalum capacitors at 5V RB).
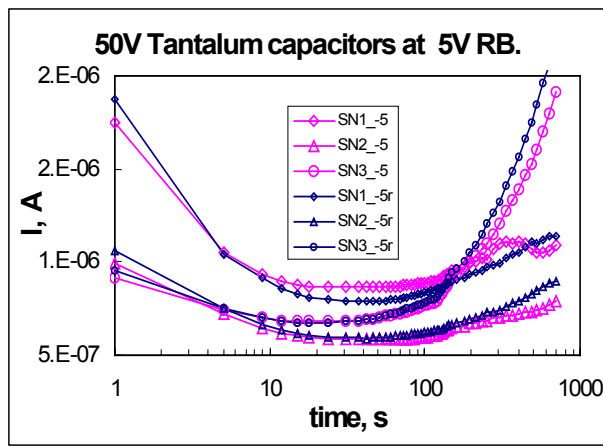
3.3. Degradation under Reverse Bias Conditions

Reverse bias leakage currents were monitored on groups of three capacitors of each voltage rating during reverse bias cycles (RBC) as it was described in the experimental section (see Figures 1b, c).

Four groups of 50V capacitors were tested at 3V, 5V, 7V, and 9V of reverse bias. The results of the test are shown in Figure 10. In all cases the currents initially declined with time during a period which decreased with increasing voltage from approximately 1000 s at 3V to 10 - 20 s at 9V. After this current-declining period, the currents gradually increased 2 to 3 orders of magnitude over several hours. Each consequent reverse bias cycle during the 3V, 5V, and 7V tests resulted in similar I vs. t curves with some decreasing of the current-declining period and increasing of the current levels. This indicated that only partial reversibility occurred during the interim forward bias measurements (FBM). The interim FBM during the 3V, 5V, and 7V tests were performed at 10V of forward bias. During the 9V test the interim measurements were performed at 50V of forward bias, which resulted in much better reproducibility of the I vs. t curves (see Figure 10d) and suggested a virtually complete reversibility of the reverse bias degradation process.
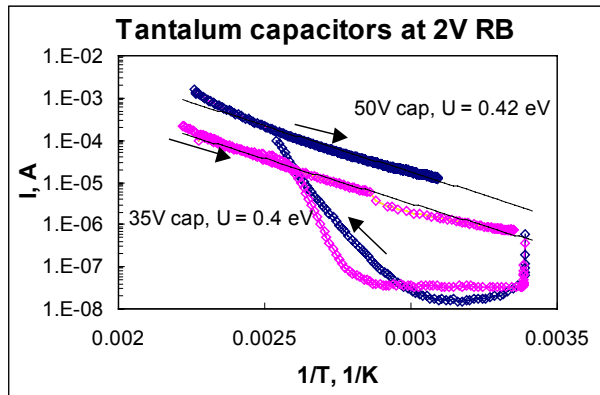

Figure 9. Arrhenius plots for a 35V and a 50V capacitors measured at 2V reverse bias and temperature range from 20 °C to 175 °C.

During the RBT of the 50 V rated capacitors one sample failed after the 10th 9V cycle (approximately 2 hours of stress) and another sample failed after the 13th cycle (12 hours of reverse bias stress). However, these failures occurred not under the reverse bias conditions, but during the interim 50V FBMs. Figure 11 shows results of these interim measurements. No significant variations from measurement to measurement were observed in the current decay up to the cycles at which the failure was observed. The failures occurred after several seconds under forward voltage due to time-dependent dielectric breakdown, thus indicating a weakening of the parts during the reverse bias stress.
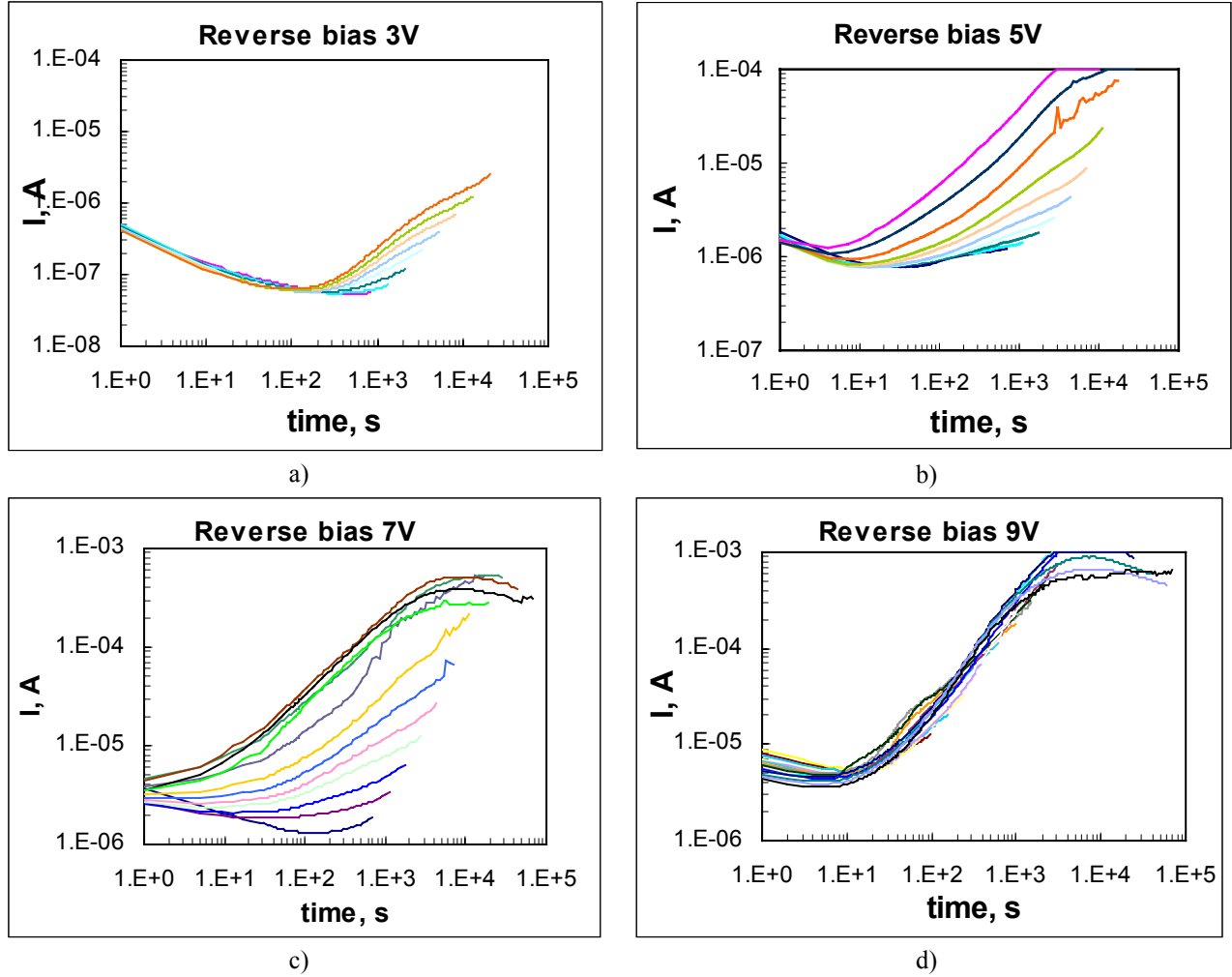
Figure 10. Reverse bias test cycles of 50V tantalum capacitors at different voltages. Different lines indicate different cycles of reverse bias stress. Note that the interim measurements during tests at 3V, 5V, and 7V were performed at a forward voltage of 10V. The interim measurements during the 9V testing were performed at 50V.

Typical time evolution of currents during the RBT cycles for the three capacitor ratings is shown in Figure 12. In all cases the currents slightly decreased with time (during 10 to 1000 seconds, which is not seen on these hours-scaled charts) following approximately 10 to 20 hours of current increase and then stabilized at somewhat lower level. Similar to what was observed in [1], the stabilization currents in many cases were not steady but exhibited erratic variations around the quasi-stabilization level. These quasi-stabilization levels observed in experiments at different reverse voltages are shown in Table 2.

In some instances at relatively high reverse voltages of approximately 20% V_R or more, the quasi stabilization levels tended to increase with time as shown in Figure 12d. In these cases the parts either eventually failed due to thermal run away or stabilized at a certain leakage current level.
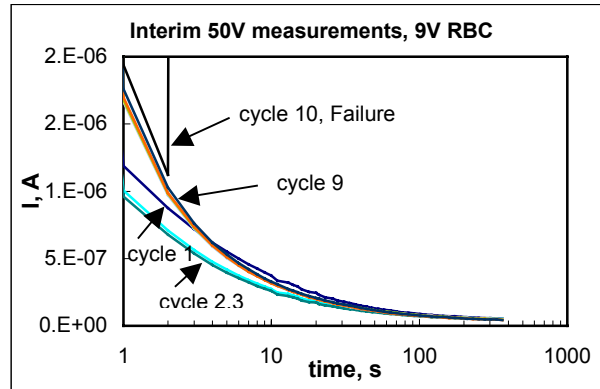
a)
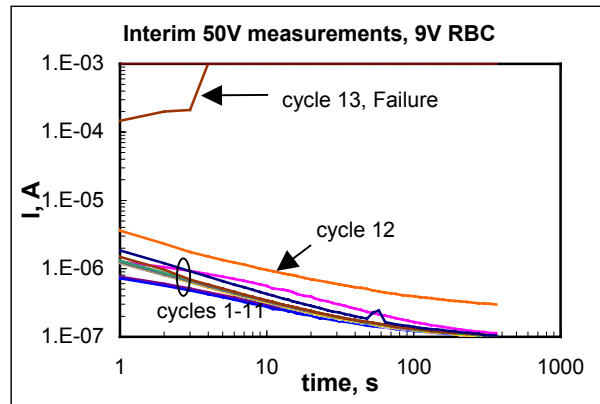
b)

Figure 11. Interim forward-bias measurements on the 50V capacitors, SN 1 (a) and SN 3 (b), performed at rated voltage during the 9V reverse bias testing.

Table 2. Levels of quasi-stabilization currents (µA) during the reverse bias tests at different voltages.

Capacitor	Reverse bias			
	3V	5V	7V	9V
20V	500-1000	5000 - 9000	-	-
35V	4-9	>1000	2000 - 5000	-
50V	2-12	>100	400-600	700 - >1000

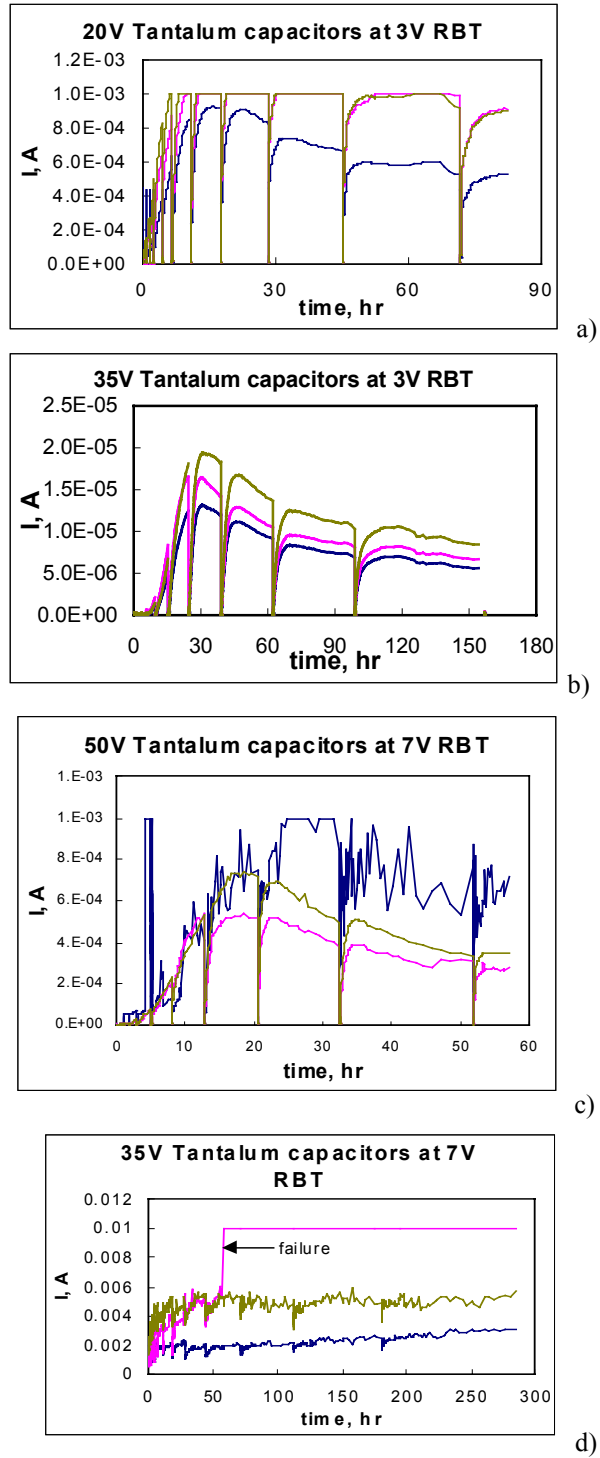Figure 12. Examples of reverse current evolution with time during reverse bias cycles for the 20V (a), 35V (b, d) and 50V (c) capacitors. For the 20V and 50V capacitors the current was limited to 1 mA.

Figure 13 displays reverse I-V characteristics measured on a 35V capacitor after a long-term (more then 100 hours) 7V reverse bias cycling stress. To decrease the effect of depolarization caused by the voltage interruption between

the testing and measurement conditions, the interim measurements were performed at reverse voltages starting at 7V (the voltage at which the parts were stressed), gradually decreasing to 0.1V and then increasing back to 7V. The I-V characteristics measured during the first few hours of the test exhibited significant hysteresis with currents at the decreasing branch of the curve being 2 to 3 orders of magnitude larger than at the increasing branch. This indicates that even a short-term decrease in the reverse voltage at early stage of the stress might reverse degradation process. After approximately 100 hours of stress, which corresponds to the 7th interim measurement cycle, the hysteresis was significantly less and the I-V curves could be roughly approximated with the power law, $I \sim V^n$, where $n \sim 1.66$. Further testing resulted in decreasing of the reverse currents at 7V by approximately an order of magnitude and, what is most interesting, in saturation of the I-V curves at $V > 1.5V$.
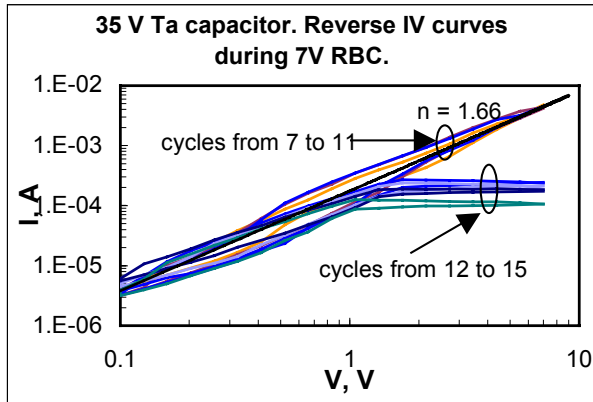

Figure 13. Interim reverse I-V characteristics of a 35V capacitor during reverse bias testing at 7V.

3.4. Reverse bias stress results at 25% and 50% VR

Two groups of 10 samples each were taken from each of the three capacitor rating lots. One group was stressed at 25% V_R and the other at 50% V_R applied in reverse direction. The reverse currents were monitored for up to 4400 hours of the testing.

Typical I vs. t curves for the testing at 50% V_R (reverse bias) are shown in Figure 14. Most of the 35V and 50V capacitors failed within first 1000 seconds of this test. The failure manifested as a sharp increase in reverse leakage currents to more than 100 mA. Subsequent measurements of the failures under forward bias conditions showed that the forward leakage currents were increased to 0.1 mA to 10 mA compared to less than 1 µA prior to the test. If a sample was not removed from the test immediately after the failure had occurred, discoloration of the plastic package was observed indicating overheating of the part. In all cases the discoloration was observed evenly around the surface of the tantalum slug. The uniform distribution of the damage suggests that the reverse bias failures occur due to an even distribution of high-density currents over the tantalum pentoxide layer. By contrast, parts that fail under forward bias conditions generally exhibit a localized failure site within the pentoxide film. Obviously, this uniformity appeared only on the macroscopic scale and most likely was due to irregularities of micrometer size which had excessive current density and were evenly distributed along the surface of the slug.
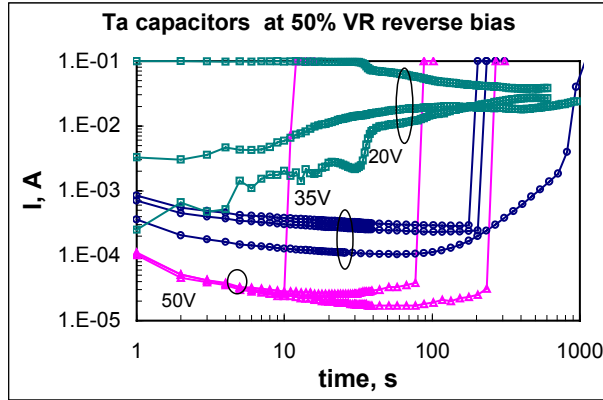
Figure 14. Typical I-t curves during reverse bias tests at 50% of rated voltage. All 35V and 50V capacitors failed with leakage currents of more than 100 mA within first several minutes of testing.

With 50% of V_R applied in reverse bias the 20V capacitors initially had rather high currents which varied within the range from 1 to 100 mA. However, no catastrophic failures were observed in this group even after 250 hours of the stress. After the test these capacitors had excessive forward leakage currents ranging from micro- to milliamperes.

Reverse currents during the 25% V_R test for the 35V and 50V capacitors significantly increased with time during the first several hours of testing and then varied erratically in the milliampere range. Figure 15 exhibits time evolution of currents for all capacitors in the 50V group. Most of the parts failed after approximately 250 hours of the stress. It is important to note that all failures occurred within 20 to 40 hours after the reverse bias was interrupted for replacement of the limiting resistors. The 100 Ohm resistors, which had been used initially for approximately 230 hours, were replaced with 10 Ohm resistors to reduce changes of the voltage across the capacitors when the currents increase above 10 mA. Comparison of currents right before and immediately after this replacement did not reveal any significant changes in reverse currents which is understandable considering that the voltage drop on the limiting resistors was decreased by the replacement from less than 4%-6% to less than 0.4%-0.6%.
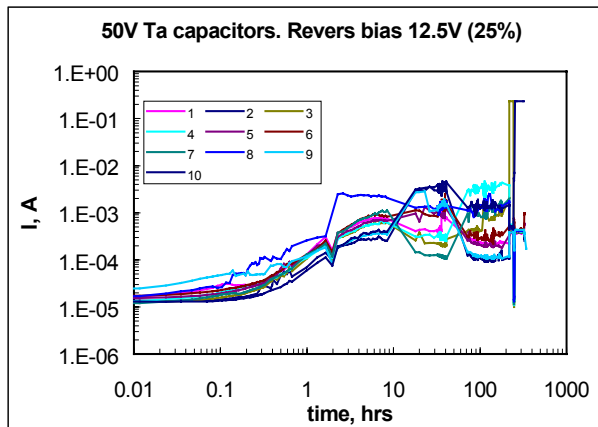
Figure 15. Reverse bias test results for ten 50V capacitors at 25% rated voltage.

The kinetics of failures for both types of capacitors are shown in Figure 16. An increase in the applied voltage from 25% V_R to 50% V_R resulted in decreasing of the median time-to-failure by more than three orders of magnitude. However, considering possible impact of the test interruption, the time-to-failure during 25% V_R test could be much larger and the difference between the 25% V_R test and the 50% V_R test could be much more dramatic.

In the 20 V group only one failure occurred after 280 hours of the 25% V_R reverse bias test (also after the testing interruption for replacement of the resistors). All other capacitors survived 2400 hrs of testing with the currents stabilizing in the range from 4 mA to 10 mA. After 2400 hours of testing four capacitors were removed for analysis and 5 remaining capacitors were stressed up to 4400 hours. After 4400 hours under bias the power supply was turned off and then turned on after approximately 15 hours. Two more parts (out of five) failed within several minutes after the power had been reapplied.

a)

b)
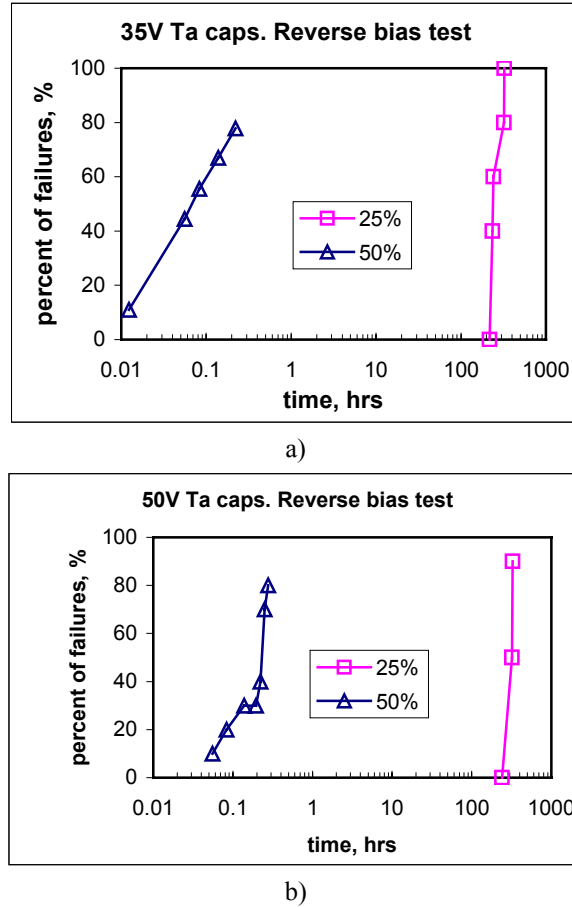
Figure 16. Kinetics of failures for 35V (a) and 50V (b) capacitors during reverse bias tests at 25% and 50% of rated voltage.

AC characteristics (capacitance at 1 kHz and ESR at 100 kHz) were measured on all capacitors, which did not fail hard short circuit, after the 25% and 50% V_R stresses. In spite of significantly increased leakage currents, no dramatic changes occurred in C and ESR values after the 50% V_R test: the values of capacitance decreased by 3% to 5% and the ESR values increased by 20% to 40%. Figure 18 shows before/after test correlation in capacitance and ESR for parts subjected to 25% V_R reverse bias testing. Here also, the capacitance decreased by a few percent and the resistance increased by 30% to 100 %. These data concur with the results reported in [1].
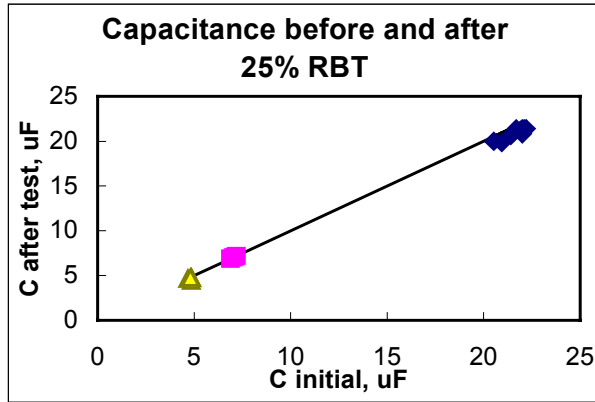
a)
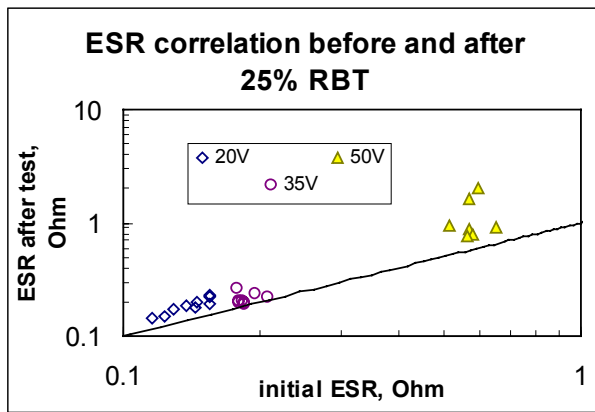
b)

Figure 17. Effect of 25%VR reverse bias testing on capacitance (a) and ESR (b) for the three types of capacitors. The lines correspond to the no-change characteristics.

Figure 18 shows changes in frequency dependencies of C and ESR for the 20V rated capacitors after 2400 hours of reverse bias at 25% V_R. Similar degradation in the frequency dependencies was observed with the 35V and 50V rated capacitors after reverse bias testing. As expected from the C and ESR measurements, no significant changes occurred at low and high frequencies. However in the range from 3 kHz to 300 kHz capacitance after the test was 25% to 50% reduced compared to the initial values. This indicates a substantial increase in the capacitance roll-off effect. This degradation was most likely caused by an increase of the resistance of the manganese dioxide layer [17, 18]. The reverse bias stress also resulted in several times increase of the ESR at frequencies below 30 kHz. This effect might be due to the increased conductivity of tantalum pentoxide layers.
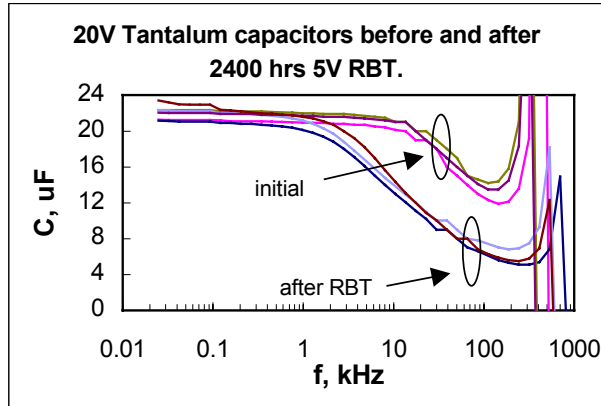
a)
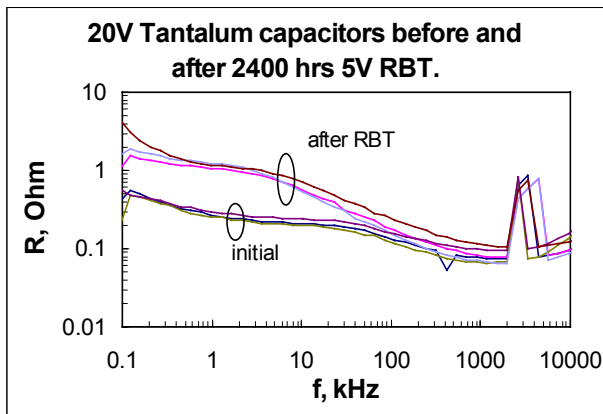
b)

Figure 18. Effect of 2400-hour reverse bias testing at 5V on AC characteristics of 20V tantalum capacitors.

A typical forward current decay in the 20V capacitors subjected to the 25% V_R testing is shown in Figure 19. The forward currents decreased with time according to the power law, $I \sim t^{-n}$, with the decay rate, n, varying from 0.26 to 0.35. Compared to the initial curves, the forward currents after the reverse bias stress were several times higher, and the rate of the decay was significantly lower. Initially, the n values were 0.75 to 0.9 but after the test they varied for different samples from 0.15 to 0.35.

4. Discussion

The observed experimental data can be explained based on physical notions of the processes in the valve metal (niobium, tantalum) – amorphous oxide (Nb_2O_5, Ta_2O_5) systems which were suggested first in [14, 15] and then later developed by one of the co-authors for solid tantalum capacitors [5, 6]. According to these notions, the Ta/Ta_2O_5 system, which is formed by anodizing tantalum, is in a thermodynamically non-equilibrium condition and relaxes to a stable state by chemical reduction-oxidation reactions at the Ta/Ta_2O_5 and MnO_2/Ta_2O_5 interfaces and related structural transformations. The relaxation is accomplished by two processes: crystallization and reduction of the Ta_2O_5 to lower oxide states. These processes were started with the formation of Ta/Ta_2O_5 interface, then accelerated during high temperature treatments at the time of manufacturing and might slowly continue during the whole life span of the capacitors.
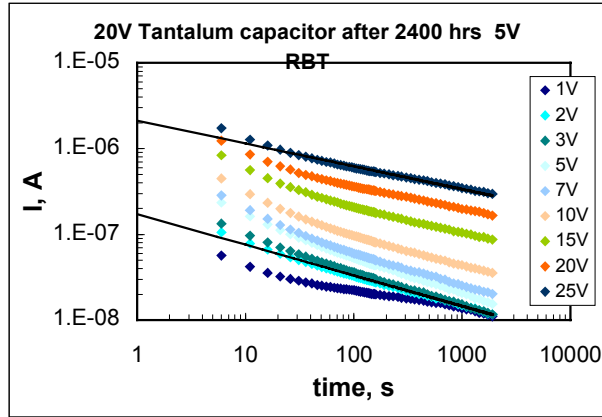
Figure 19. Typical polarization curves after long-term reverse bias testing. The slope of the lines varied from 0.27 to 0.33

4.1. Conduction Mechanism in Forward-biased Tantalum Capacitors

Under normal operating conditions, oxygen ions from a Ta_2O_5 film move into the bulk Ta thus decreasing the internal energy of the system and leaving positively charged oxygen vacancies, V_O^+ , in the oxide near the tantalum surface. Under electrical field in the oxide these vacancies migrate towards the Ta_2O_5/MnO_2 interface. The MnO_2, being a strong oxidizer, easily emits oxygen ions which recombine with the arrived oxygen vacancies. The process is controlled by the V_O^+ generation and might proceed with crystallization of the oxide film forming conductive TaO inclusions at the Ta/Ta_2O_5 interface. The probability of the inclusion formation strongly depends on the quality of the tantalum anode and, in particular, on the oxygen content and on existence of the thermal oxide layer under the anodized tantalum pentoxide.

The ionic currents caused by the V_O^+ and O^- migration could be large enough at high temperatures, above approximately 250 °C, and are responsible for the galvanic cell properties of the $Ta/Ta_2O_5/MnO_2$ system. The activation energy of the ionic currents is relatively high, ~ 1.85 eV, so the level of ionic currents at temperatures below 150 °C is negligibly small. Crystallization in tantalum oxide films was observed at a high temperature of 480 °C after 5-60 minutes of annealing in air on Ta films saturated with oxygen. This process occurs in a thermal oxide layer, which is formed under the anodic oxide and is much less resistant to crystallization [19]. At normal operating conditions of tantalum capacitors both relaxation processes, the reduction of the tantalum pentoxide and crystallization at the Ta/Ta_2O_5 interface, occur extremely slowly and the ionic subsystem (oxygen vacancies and oxygen ions) virtually does not affect the behavior of the electronic subsystem.

Within the range of operation temperatures of tantalum capacitors the dominant conduction mechanism is related to electron migration in tantalum pentoxide layers. This migration occurs via electron hopping transport, resulting in the absorption currents, and via Pool-Frenkel mechanism resulting in the conduction currents. The first mechanism is mostly dependant on volume properties of the tantalum pentoxide layer (traps' concentration and distribution) whereas the second one is controlled by the Ta_2O_5/MnO_2 and/or Ta/Ta_2O_5 interface conditions (work function and local electric field). The sites of the interfaces with some structural irregularities, which increase local electric field in the pentoxide layer and/or decreased work function for electron emission, are most likely favorable for the Pool-Frenkel transport mechanism. Combination of these two mechanisms can explain time-, voltage-, and temperature evolution of the forward bias leakage currents. The first mechanism prevails at relatively low temperatures and voltages while the second one dominates at high temperatures and voltages.

4.2. Mechanism of Reverse Bias Degradation

As it was shown in our experiments, a characteristic feature of reverse currents in tantalum capacitors is gradual increase with time (for several hours) following a relatively short period of current decrease. A typical time

evolution of reverse currents includes three stages: current decay, gradual current increase, and erratic behavior when the currents quasi-stabilize. This suggests three different processes governing degradation in reverse biased tantalum capacitors during these three periods.

First stage. At relatively low reverse voltages polarization and depolarization kinetics is similar to what was observed at forward voltages. This indicates that during the first stage the current decay is most likely due to the same mechanisms that control forward biased currents.

Second stage. The gradual increase of reverse currents during the second stage can be explained by accumulation of the oxygen vacancies at the tantalum cathode. Unlike the forward bias conditions, the positively charged oxygen vacancies generated at the Ta/Ta_2O_5 interface do not migrate toward the MnO_2 layer, but are piling up at the tantalum electrode. Besides, oxygen vacancies existing in the bulk of the oxide layer also will be swept toward the Ta/Ta_2O_5 interface by the applied reverse bias. Accumulation of the positively charged oxygen vacancies reduces the barrier for electron emission into the oxide and provides additional traps for electrons in the oxide thus resulting in significant increase of reverse currents.

Third stage. A high level of electron emission from the Ta cathode occurs preferably at irregularities at the Ta/Ta_2O_5 interface. Under reverse bias conditions these local currents increase with time to the level which is sufficient to overheat micro-sites in the opposed MnO_2 layer. This local overheating will cause oxygen emission from the MnO_2 layer and its reduction to the lower level, high resistive oxides (Mn_2O_3). Both processes, the oxygen emission and the manganese reduction, will reduce local reverse currents and result in quasi-stabilization in the system. The first, by supplying oxygen through diffusion in Ta_2O_5 and neutralizing positively charged oxygen vacancies. The second process by limiting the reverse currents due to increased resistivity of manganese layer (well-known self-healing mechanism). The reduction of manganese also explains the observed increase of the roll-off effect in capacitors (see Figure 18). Both processes occur locally at different points in time and are most likely responsible for the erratic variation of currents during the third stage of the reverse bias stress.

Another possible mechanism, which results in decreasing and stabilizing of reverse currents, is electron trapping at states related to oxygen vacancies at the Ta/Ta_2O_5 interface. This trapping reduces the effective positive charge and thus decreases the emission of electrons from the tantalum cathode.

At the first and second stages the degradation process still might be completely reversible. Application of a forward bias would sweep the oxygen vacancies to the Ta_2O_5/MnO_2 interface where they would be neutralized by oxygen ions from the MnO_2 layer as it occurs under normal operating conditions. Similar relaxation would occur even during depolarization without applying of forward voltage due to diffusion of the oxygen vacancies and/or their migration in the internal electrical field in the tantalum pentoxide layer.

Experiments have shown that restoration of characteristics of capacitors after the bias reversal from reverse to forward occurs very fast, within a few seconds or less. This allows an estimation of the mobility of oxygen vacancies in Ta_2O_5 using the following expression:

$$\mu = \frac{d^2}{V \times t} \quad ,$$

where d is the thickness of the oxide; V is the applied voltage; t is the time of the migration. For rough estimations we can assume the oxide thickness d = 200 nm, the applied voltage V = 10 V, and the duration of the transport t = 10 s. The calculation yields
$\mu = 4 \times 10^{-12}$ cm^2/(V×s).

A relatively high mobility of oxygen vacancies in ceramics was shown in [16]. Experiments with the perovskite-type titanates showed that the mobility of the oxygen vacancies was $(1 – 6) \times 10^{-8}$ cm^2/Vs at temperatures of 160 - 190 °C. Considering relatively high activation energy for ions, the mobility of oxygen vacancies at room temperature would be several orders of magnitude lower, which is in reasonable agreement with our estimations.

At high reverse voltages the accumulation of oxygen vacancies increases local currents to the level where they might be limited by the emission capability of the tantalum cathode. In this case the appearance of the reverse I-V curves (see Figure 13) is similar to the forward characteristics of vacuum diodes. In a vacuum diode forward currents first increase with voltage according to the Child and Langmuir 3/2 law ($I \sim V^{3/2}$) and then saturate at levels which exponentially depend on the cathode temperature.

A weakening of the electrical strength of the dielectric layers in solid tantalum capacitors was also observed after long-term testing under reverse bias conditions (see Figure 11). This might be due to crystallization of the tantalum pentoxide which is facilitated by excessive concentration of oxygen vacancies at the Ta/Ta_2O_5 interface and increased local temperature at existing irregularities. The excessive V_O^+ concentration and related electron traps were also likely responsible for the increased absorption currents and decreased rate of the current decay after long-term reverse bias testing (see Figure 19).

An interesting feature of the behavior of reverse biased capacitors during the third stage of degradation is an initiation of failures by the bias interruption. In several instances hard failures of the capacitors occurred in time ranging from a few minutes to a few hours after the voltage was turned off and then reapplied. This effect can be explained assuming that after the reverse bias is turned off the oxygen vacancies, V_O^+, diffuse from the Ta/Ta_2O_5 interface into the oxide and then, after the bias is reapplied, redistribute back to the interface. Originally, oxygen vacancies were generated more or less evenly along the Ta/Ta_2O_5 interface, however after voltage reapplication they would mostly concentrate at sites with structural irregularities where the electrical field is larger. Similar redistribution would result in higher than original concentration of the positively charged vacancies at the irregularities thus increasing the electron emission to the level when destruction of the oxide and a hard failure of the capacitor would occur.

Another possible mechanism of these triggered-by-interruption failures is related to the processes of electron capture and emission from the V_O^+-related traps. The voltage removal will cause emission of the trapped electrons from the states at the Ta/Ta_2O_5 interface thus increasing the effective positive charge created by oxygen vacancies. After reapplying of the reverse voltage, retrapping of the electrons would take some time during which the effective positive charge and correspondingly the local current density would be higher that they had been before the voltage interruption.

4.3. Factors affecting failures in systems with inversely inserted Ta capacitors

Experiments showed that reverse bias stresses during 10 to 20 hours even at relatively low voltages would increase forward leakage currents above the specification limits which signifies a formal failure of the capacitor. However for a system with inversely inserted capacitors the level of forward leakage currents is not important and the failure condition (the critical level of reverse current) should be determined specifically for each application condition.

Depending on external and material parameters of tantalum capacitors, a reverse bias current can either degrade to a level after which a thermal runaway would occur, or it might stabilize at a certain level exhibiting erratic current variations. In the first case a hard short in the capacitor and consequently a failure of the system would occur. In the second case one might expect some degradation of AC characteristics (relatively minor decrease in C, increase in ESR and in the roll-off effect) and substantial increase in the leakage currents (up to tens of milliamperes). However, no hard short circuit failures would happen for thousand of hours provided the system can remain operational at high levels of leakage currents. It should be noted that in this case, the leakage currents will not be stable and the reversed biased capacitors would generate significant noise possibly resulting in malfunctions in sensitive circuits.

The external parameters that affect reverse bias behavior of tantalum capacitors include applied voltage, temperature, thermal resistance, and specific features of the circuit application, in particular limiting current in the circuit and the probability of bias interruption.

Reverse voltage. In systems with virtually unlimited current supply (typically for tantalum capacitors used in power lines) an increase in reverse voltage would significantly increase the probability of hard failures starting from a certain threshold voltage, V^r_{th}. Below this voltage capacitors can withstand thousand of hours of uninterrupted operation without hard failures. Based on our experiments this threshold voltage is expected to be somewhere between 15% and 25% of the rated voltages. Most likely for capacitors rated for 35V and 50V this threshold is closer to 15%, whereas for the 20V capacitors it is above 25%. This means in particular that all capacitors rated above 20V would most likely withstand thousand of hours being inversely installed in a 5Vpower bus system.

It should be noted that the suggested model and the observed results do not allow relating directly the reverse current degradation to the rated voltage of capacitors or to the thickness of the pentoxide layer. It is quite possible that the threshold voltage V^r_{th} is specific for a given lot of capacitors and cannot be determined in terms of percentage of V_R in a general case.

Obviously, capacitors rated for low voltages at the same current levels and derating conditions, would dissipate less power compared to the high voltage capacitors and thus would be less prone to thermal runaway and failures. This might be one of the reasons for better performance of the 20V capacitors in our tests. Another reason could be a slower crystallization process in capacitors with thin tantalum pentoxide films compared to high voltage capacitors with relatively thick oxide films [19].

Limiting current. The level of limiting current strongly affects the probability of hard failures under reverse bias conditions. In this respect the behavior of tantalum capacitors is similar to behavior of forward biased diodes. Similar to forward-biased diodes, hard failures in reverse biased capacitors are also caused by a thermal runaway, the probability of which depends on the current available in the circuit and the thermal resistance of the part. If a capacitor is used to filter input or output signals in a microcircuit, the available current most likely will be low (milliamperes or less). In this case the initial voltage at the capacitor can be much higher than the threshold voltage V^r_{th}, which is determined for unlimited current conditions, and can reach up to 100% V_R. The leakage current in such a capacitor would relatively quickly (during a few hours) increase to the level limited by the external circuit. This would decrease the voltage drop across the capacitor thus limiting the power dissipated in the part and preventing its catastrophic failure.

Temperature and thermal resistance. Hard failures in inversely installed tantalum capacitors are due to thermal run-away caused by increased currents more-or-less evenly distributed along the tantalum slug. Typically tantalum chip capacitors in normal mounting configurations have thermal resistance of $R_{th} \approx 100$ °C/W. This limits the dissipation power to approximately 1 Watt (assuming that temperature increase above 125 °C will cause thermal runaway in the capacitor). An increase in ambient temperature, T_a, and/or increase in R_{th}, (due for example to use in a vacuum or degradation of attachment to the board) would raise the temperature of a capacitor, $T = T_a + P*R_{th}$ and cause failure at a lower level of power.

Bias interruptions during operation. Power interruptions at early stages of degradation under reverse bias conditions (the 1st and the 2nd stages) would result in charge relaxation at the Ta/Ta$_2$O$_5$ interface to original conditions and thus might be considered as benign. However similar interruptions after a long-term reverse bias stress (the 3rd stage of reverse bias degradation) would significantly increase the probability of failures. In this case hard failures could be expected within minutes or hours after switching due to the triggered-by-interruption failure mechanism discussed above.

According to the described model of degradation, the most important material parameters of capacitors affecting their robustness under reverse bias conditions are the initial concentration of oxygen vacancies in the tantalum pentoxide layer and the rate of their generation at the Ta / Ta$_2$O$_5$ interface. The latter most likely depends on purity of the tantalum slug and, in particular, on concentration of oxygen. Obviously, these parameters depend on the used materials and on manufacturing processes and are lot related as it was observed in [1, 2]. Unfortunately there is no established correlation between the material parameters and characteristics of capacitors, which explains difficulties in predicting their reliability under reverse bias conditions.

5. Conclusions

1. At relatively low voltages, below 50% V_R, the kinetics of reverse bias currents features three stages. The first is a relatively short (tens to thousands of seconds) period when currents decrease with time. During the second, hours-scaled stage, currents gradually increase approximately two to three orders of magnitude. Then, during the third stage, currents often exhibit erratic behavior and either reach maximum, after which they are quasi-stabilizing at somewhat lower levels, or continue to increase erratically. In the latter case the part eventually fails due to a thermal run-away.

2. In spite of significant increase in currents during the second stage of reverse bias stress, the initial forward and reverse characteristics of the capacitors can be restored after a few minutes of depolarization and/or several seconds of forward bias polarization. Irreversible degradation in capacitors occurs during the third stage and results in a weakening of the electrical strength of the tantalum pentoxide layer and in increasing of the capacitance roll-off effect. The AC parameters of capacitors (C at 1 kHz and ESR at 100 kHz) experienced relatively minor changes.

3. The experimental results suggest the existence of a threshold voltage above which tantalum capacitors installed backwards would fail within seconds, and below which they would withstand hundreds and thousands of

hours enduring relatively high leakage currents (in the milliampere range) but without hard failures. Depending on the type of capacitor this threshold voltage is probably between 15% and 25% of the rated voltages.

4. The probability of hard failures in tantalum capacitors, which are installed in a reverse bias orientation on a board, depends on application and, in particular, on the level of limiting current in the circuit. Interruptions of applied voltage might increase significantly the probability of failures. In applications where the current is limited to a few milliamperes or less, the initial voltage can be much larger than the threshold voltage and the limiting level of leakage will be reached within a few hours. Although no hard failures occur in this case, the reverse currents are varying erratically creating significant noise which can cause malfunctions in sensitive circuits.

5. The behavior of forward polarization and depolarization currents has been explained assuming that the forward current is a sum of the absorption current, which varies with time according to the power law, and the conductivity current, which does not depend on time. The absorption currents are due to electron trap hopping transport. The Pool-Frenkel mechanism controls the conduction currents, which strongly depend on applied voltage and temperature and have activation energy of 0.5-0.75 eV. These currents are dominant at high voltage and temperature conditions.

6. A mechanism of degradation in reverse biased tantalum capacitors and factors affecting failures in systems with inversely installed capacitors has been discussed. The 3-stage evolution of reverse currents has been explained based on generation and migration of oxygen vacancies in $Ta/Ta_2O_5./MnO_2$ structures.

6. References

1. G.J.Ewell, Reverse bias characteristics of solid tantalum capacitors, CARTS'84, pp. 21- 51, 1984.

2. M.J.Cozzolino, R.C.Straessle, Design, characteristics, and failure mechanisms of tantalum capacitors, CARTS'88, pp. 98-110, 1988.

3. I.Bishop and J.Gill, Reverse voltage behavior of solid tantalum capacitors, AVX Technical information, http://www.avxcorp.com.

4. J.Sikula, J.Pavelka, J.Hlavka, V.Sedlakova, L.Grmela, The tantalum capacitor as a MIS structure in reverse mode, CARTS'01, pp. 289-292, 2001.

5. Y.Pozdeev-Freeman, Physical principles of the solid tantalum capacitors, CARTS'97, pp. 161-165, 1997.

6. Y.Pozdeev-Freeman, Battle for high CV tantalum capacitors, CARTS'01, pp. 35 -39, 2001.

7. S.Duenas, H.Castan, J.Barbolla, R.R.Kola, P.A.Sullivan, Electrical characteristics of anodic tantalum pentoxide thin films under thermal stress, Microelectronics reliability, 40, (2000), pp. 659-62.

8. S.Ang, W.Brown, Tantalum oxide dielectric for embedded capacitor applications, Proc. Of the 6th International conf. On properties and applications of dielectric materials, pp. 841-844, 2000.

9. G.Oehrlein, Oxidation temperature dependence on the dc electrical conduction characteristics and dielectric strength of thin Ta2O5 films on silicon, J.Appl. Phys, 59 (5), March 1986, pp. 1587-1595.

10. S.Khanin, Hopping electronic conduction in metal oxide films and their insulating properties, Conduction and Breakdown in Solid Dielectrics, 1992., Proceedings of the 4th International Conference on , 1992, Page(s): 57 – 61.

11. R.Franklin, Analysis of solid tantalum capacitor leakage current, AVX Technical information, http://www.avxcorp.com.

12. P.K.Watson, The transport and trapping of electrons in polymers, Electrical Insulation and Dielectric Phenomena, 1995. Annual Report., Conference on , 1995, Page(s): 21 –27

13. S.Khanin, Polaronic effects in disordered dielectrics, 9th International Symposium on Electrets, 1996. (ISE 9), Page(s): 93 –98.

14. B.T.Boiko, P.A.Pachena, V.R.Kopach, Y.L.Pozdeev, Transformation in a metal/insulator/semiconductor structure with an amorphous insulator film caused by contacts, Thin solid films, 130 (1985), pp.341-355.

15. B.T.Boiko, V.R.Kopach, S.M.Melentjev, P.A.Pachena, Y.L.Pozdeev, V.V.Starikov, Comparison of the degradation modes in sandwich structures including amorphous oxides of niobium and tantalum, Thin solid films, 229 (1993), pp.207-215.

16.   R.Waser, T.Baiatu, K.Hardtl, DC electrical degradation of pervoskite-type titanates Ceramics, J. Am. Ceram. Soc., v.73 [6], pp. 1645 – 1662, 1990.

17.   E.K.Reed, J.C.Marshall, 18 milliohms and falling – new ultra low ESR tantalum chip capacitors, CARTS'99, pp. 133 -141, 1999.

18.   J.D.Prymak, Replacing MnO2 with conductive polymer in solid tantalum capacitors, CARTS'99, pp. 148 - 153, 1999.

19.   Y.Pozdeev-Freeman, A. Gladkish, New problems and new decisions for low voltage high CV tantalum capacitors, CARTS'99, pp. 142 -147, 1999.

7. Acknowledgments